DMD Fast Forward. Published on December 22, 2010 as doi:10.1124/dmd.110.036418

DMD # 36418

In Vitro Metabolism of 17-(dimethylaminoethylamino)-17-demethoxygeldanamycin (17-DMAG) in Human Liver Microsomes

Nan Zheng, Peng Zou, Shaomeng Wang, and Duxin Sun

Department of Pharmaceutical Sciences, College of Pharmacy, University of Michigan, Ann Arbor, Michigan (N.Z., P.Z., D.S.), Departments of Internal Medicine and Medicinal Chemistry and Comprehensive Cancer Center, University of Michigan, Ann Arbor, Michigan (S.W.)

Running Title: *In vitro* metabolism of 17-DMAG in human liver microsomes

Address correspondence to:

Duxin Sun, PhD

Department of Pharmaceutical Sciences, College of Pharmacy, The University of Michigan, 428 Church Street, Ann Arbor, MI 48109, Tel: 734-615-8740, Fax: 734-615-6162 Email: duxins@umich.edu

Number of text pages: 28

Number of tables: 0

Number of figures: 9

Number of references: 31

Number of words in the Abstract: 180

Number of words in the Introduction: 520

Number of words in the Discussion: 1,351

ABBREVIATIONS: 17-DMAG, 17-(dimethylaminoethylamino)-17-demethoxy geldanamycin; GA, geldanamycin; Hsp90, heat shock protein 90; HLMs, human liver microsomes; 17-AAG, 17-(allylamino)-17-demethoxygeldanamycin; GAH_2, geldanamycin hydroquinone; GSH, glutathione; 17-AG, 17-Aminogeldanamycin; GA-SG, 19-glutathionyl geldanamycin; GAH_2-SG, 19-glutathionyl geldanamycin hydroquinone; 17-$AAGH_2$,17-(allylamino)-17-demethoxygeldanamycin hydroquinone; 17-AAG-SG, 19-glutathionyl 17-(allylamino)-17-demethoxygeldanamycin; 17-$AAGH_2$-SG, 19-glutathionyl 17-(allylamino)-17-demethoxygeldanamycin hydroquinone; 17-$DMAGH_2$, 17-(dimethylaminoethylamino)-17-demethoxygeldanamycin hydroquinone;

17-DMAG-SG, 19-glutathionyl 17-(dimethylaminoethylamino)-17-demethoxy geldanamycin; 17-DMAGH_2-SG; 19-glutathionyl 17-(dimethylaminoethylamino)-17-demethoxygeldanamycin hydroquinone; Mr, protonated molecular ion; MRM, multiple reaction monitoring; EPI, enhanced product ion.

Abstract

The objective of this study was to investigate the oxidative metabolism pathways of 17-(dimethylaminoethylamino)-17-demethoxygeldanamycin (17-DMAG), a geldanamycin (GA) derivative and Hsp90 inhibitor. *In vitro* metabolic profiles of 17-DMAG were examined by using pooled human liver microsomes (HLMs) and recombinant CYP450 isozymes in the presence or absence of reduced glutathione. In addition to 17-DMAG hydroquinone and 19-glutathionyl 17-DMAG, several oxidative metabolites of 17-DMAG were detected and characterized by liquid chromatography-tandem mass spectrometry. Different from previously reported primary biotransformations of GA and GA derivatives, 17-DMAG was not primarily metabolized through the reduction of benzoquinone and glutathione conjugation in HLMs. In contrast, the primary biotransformations of 17-DMAG in HLMs were hydroxylation and demethylation on its side chains. The most abundant metabolite was produced by demethylation from the methoxyl at position 12. The reaction phenotyping study showed that CYP3A4 and 3A5 were the major P450 isozymes involved in the oxidative metabolism of 17-DMAG while CYP 2C8, 2D6 2A6, 2C19 and 1A2 made minor contributions to the formation of metabolites. Based on the identified metabolite profiles, the biotransformation pathways for 17-DMAG in HLMs were proposed.

Introduction

Hsp90 is a molecular chaperone to mediate the folding, activation and assembly of many oncogenic client proteins, which stimulate cancer cell growth (McIlwrath et al., 1996). Geldanamycin (GA) is an Hsp90 inhibitor, that binds to HSP90 and disrupts the interaction between HSP90 and its client proteins (An et al., 1997). This disruption depletes the oncogenic proteins and results in antitumor activity. To develop potent antitumor agents, a number of GA derivatives have been synthesized and characterized biologically. Among GA derivatives, 17-(allylamino)-17-demethoxygeldanamycin (17-AAG) and 17-(dimethylaminoethylamino)-17-demethoxygeldanamycin (17-DMAG) have been introduced into clinical trials (Glaze et al., 2005).

Both GA and 17-AAG are known to undergo extensive metabolism (Egorin et al., 1998; Musser et al., 2003; Guo et al., 2005; Guo et al., 2006; Lang et al., 2007). Although GA and 17-AAG are structurally similar (Figure 1), their metabolite profiles in liver microsomes are different (Lang et al., 2007). GA is primarily (40-73%) reduced into geldanamycin hydroquinone (GAH_2) (Lang et al., 2007; Guo et al., 2008). On exposure to oxygen, GAH_2 slowly reverts to GA. In the presence of reduced glutathione (GSH), more than 50% of GA is rapidly converted into 19-glutathionyl geldanamycin hydroquinone (Cysyk et al., 2006; Lang et al., 2007). No significant amount of oxidative metabolites of GA in the incubations with human liver microsomes (HLMs) has been detected (Lang et al., 2007). The metabolic pathways of 17-AAG in liver microsomes are controversial. Guo *et al.* reported that quinone/hydroquinone conversion was the primary metabolism mode of 17-AAG and 17-DMAG in microsomal preparation (Guo et

al., 2008). In the presence of reduced GSH, 15% of 17-AAG was conjugated with GSH after incubation in liver microsomes for 24 h. However, Lang *et al.* observed that only 2% of 17-AAG was reduced into hydroquinone in HLMs and no significant amount of 19-glutathione conjugate of 17-AAG was detected in HLMs in the presence of 5 mM of glutathione (Lang et al., 2007). Furthermore, they found that, different from GA, 17-AAG in HLMs primarily underwent oxidative metabolism on the 17-allylamino side chain to form 17-Aminogeldanamycin (17-AG) (Figure 1) and 17-(2',3'-Dihydroxypropylamino)-Geldanamycin, which was consistent with a previous study (Egorin et al., 1998).

17-DMAG is much more metabolically stable than 17-AAG due the limited oxidative metabolism on 17-dimethylaminoethylamino side chain (Glaze et al., 2005). Compared with 17-AAG, 17-DMAG exhibits a longer terminal half-life of 16 - 19 h (Hwang et al., 2006; Moreno-Farre et al., 2006) (4 h for 17-AAG) and a lower total clearance of 7.4 – 17.7 L/h (Hwang et al., 2006; Moreno-Farre et al., 2006) (36 L/h for 17-AAG) in human. Although the preclinical (Egorin et al., 2002) and clinical (Glaze et al., 2005; Goetz et al., 2005) pharmacokinetics of 17-DMAG have been investigated, to our knowledge, the biotransformation information of 17-DMAG is still limited and controversial. Reduction of quinone was proposed to be the primary metabolism of 17-DMAG in liver microsomes and 17-DMAG was observed to undergo more rapid GSH conjugation than 17-AAG (Guo et al., 2008). However, these findings cannot explain the less *in vivo* metabolism of 17-DMAG than that of 17-AAG in animal and human (Musser et al., 2003; Hwang et al., 2006).

Biotransformation of GA and its derivatives is related to their antitumor activity and toxicity. For example, the reduction of benzoquinone ansamycins into hydroquinone ansamycins enhanced Hsp90 inhibition (Guo et al., 2006; Lang et al., 2007) while GSH conjugation of benzoquinone ansamycins was correlated with their hepatic toxicity (Guo et al., 2008). Hence, it is important to elucidate the major biotransformation pathways of 17-DMAG in liver microsomes for discovery of more stable, potent and less toxic geldanamycin analogs.

In this study, we investigated the biotransformation pathways of 17-DMAG in HLMs and especially focused on quinone-hydroquinone conversion and GSH conjugation. The relative percentages of major metabolites of 17-DMAG were estimated by normalizing their peak areas. The major metabolites in incubations were tentatively characterized using liquid chromatography tandem mass spectrometry (LC-MS/MS) and the P450 enzymes responsible for the formation of the metabolites were identified. Based on the identified metabolite profiles, the biotransformation pathways for 17-DMAG in HLMs were proposed.

Materials and Methods

Materials. GA, 17-AAG, 17-DMAG were purchased from LC Laboratories (Woburn, MA). Reduced glutathione, reduced β-NADPH, $MgCl_2$, 0.1 M phosphate buffer, formic acid α-naphthoflavone, tranylcypromine, quercetin, sulfaphenazole, ticlopidine, diethyldithiocarbamate, quinidine and ketoconazole were supplied by Sigma-Aldrich (St. Louis, MO). MI-63 was obtained from Professor Shaomeng Wang (Department of Medicinal Chemistry, University of Michigan, Ann Arbor, MI). HPLC grade acetonitrile was purchased from Fisher Scientific (Pittsburgh, PA). HPLC water was purified using a MilliQ water system (Bedford, MA). Pooled HLMs (20 mg/ml), purified *E. coli* expressed recombinant human cytochrome P450 enzymes coexpressed with human cytochrome b_5 (1 nmol/vial) and *E. coli* expressed control microsomes were obtained from XenoTech, LLC. (Lenexa, KS).

Metabolic Stability Assay. GA, 17-AAG or 17-DMAG was incubated with HLMs in the absence or presence of reduced GSH at 37°C. The enzymes were activated by reduced β-NADPH. The incubation solution was diluted with 0.1 M phosphate buffer (containing $MgCl_2$) to 0.6 mL. The final concentrations of drug, microsomes, β-NADPH, phosphate buffer and $MgCl_2$ were 5 µM, 1 mg/ml, 1 mM, 0.1 M, and 3.3 mM respectively. For GSH conjugation assays, the final concentration of reduce GSH was 5 mM(Lang et al., 2007). An aliquot of 40 µl of mixture was collected at 1, 5, 10, 15, 30, 45, 60 and 120 min, and then proteins were precipitated with 120 µl of ice-cold acetonitrile containing an internal standard MI-63 (100 ng/ml). The samples were centrifuged at 14,000 rpm × 5 min and 10 µl of supernatant was injected into LC-MS. To determine the apparent K_m values for

the formation of 17-AG from 17-AAG, various concentrations of 17-AAG (1 – 200 μM) were incubated in 0.25 mg/ml of HLMs for 15 min in triplicate. Similarly, to determine the K_m values for the formation of M1 and M3 from 17-DMAG, various concentrations of 17-AAG (0.5 – 100 μM) were incubated in 0.5 mg/ml of HLMs for 30 min in triplicate. The formation rates of the metabolites were fitted with the Michaelis-Menten equation using WinNonlin (Pharsight Corporation, Mountain View, CA).

Incubations with HLMs for Metabolite Identification. 17-DMAG was incubated with HLMs in 0.6 ml of 0.1 M phosphate buffer at 37°C. The final concentrations of microsomes, β-NADPH, phosphate buffer and $MgCl_2$ were the same as described in stability assay. The initial concentration of 17-DMAG was 10 μM. Two different negative controls were prepared simultaneously by using boiled microsomes (100ºC for 5 min) or spiking 10 uM 17-DMAG after protein precipitation. Both samples and negative controls were incubated for 2 h and the reaction was terminated with 1.2 mL of ice-cold acetonitrile to precipitate proteins. In addition, to evaluate GSH conjugation, 17-DMAG (10 μM) was incubated with reduced GSH (5 mM) and β-NADPH (1 mM) in 0.1 M phosphate buffer (containing $MgCl_2$) in the presence or absence of HLMs (1 mg/ml) at 37°C for 2 h. After protein precipitation, samples and negative controls were centrifuged at 14,000 rpm × 5 min for LC-MS analysis.

LC-MS/MS. An Agilent 1200 HPLC system was used for separation. The processed samples were injected on a Zobarx SB-C18 column (2.1 mm × 50 mm, 3.5 μm). Mobile phase A, 0.1% formic acid and 10 mM ammonium formate in water, and mobile phase

B, 0.1% formic acid in acetonitrile, were used for a linear gradient elution as follows: 10 to 90% B in 10 min, hold 90% B for 3 min, return to 10% B in 0.1 min and hold 10% B for 3.9 min to equilibrate the column. The flow rate was 0.4 ml/min. Mass spectrometric detection was performed on a QTRAP 3200 mass spectrometer (Applied Biosystems, MDS Sciex Toronto, Canada) equipped with electrospray ionization (ESI) source. 17-DMAG was detected under positive ionization mode while 17-AAG and GA were detected under negative ionization mode. The multiple reaction monitoring (MRM) ion transition was *m/z* 617 → 58 for 17-DMAG, *m/z* 559 → 516 for GA and *m/z* 584 → 541 for 17-AAG (Smith et al., 2004). Ionization source temperature was set as 650 °C. Curtain gas, gas 1 and gas 2 were set at 30, 50 and 50 arbitrary units, respectively. Ion spray voltage was set at 5500 for 17-DMAG and -4500 for GA and 17-AAG. A neutral loss of 43 Da was observed, likely due to the loss of N-methylenemethanamine from 17 side chain. Hence, the MRM ion transitions at *m/z* 561 → 518, 864 → 821 and 866 → 823 were used to detect GA hydroquinone (GAH_2), 19-glutathionyl GA (GA-SG), and 19-glutathionyl GA hydroquinone (GAH_2-SG), respectively. MRM ion transitions at *m/z* 586 → 543, 889 → 846, 891 → 848 were utilized to detect 17-AAG hydroquinone (17-$AAGH_2$), 19-glutathionyl 17-AAG (17-AAG-SG), and 19-glutathionyl 17-AAG hydroquinone (17-$AAGH_2$-SG), respectively. Meanwhile, the tertiary amine of 17-DMAG facilitated its protonation and resulted in a high MS sensitivity under positive ionization. As a result, MRM ion transitions at *m/z* 619 → 58, 922 → 58, and 924 → 58 were used to detect 17-DMAG hydroquinone (17-$DMAGH_2$), 19-glutathionyl 17-DMAG (17-DMAG-SG), and 19-glutathionyl 17-DMAG hydroquinone (17-$DMAGH_2$-SG), respectively.

Screening and Characterization of Metabolites. GA, 17-AAG and 17-DMAG were infused into mass spectrometer to obtain their MS, MS^2 and MS^3 spectra. Based on the similarities and difference among their mass spectra, the structures of fragment ions of protonated 17-DMAG were tentatively proposed. MRM ion transitions 617 → 58, 617.3 → 159 and 617 → 524 were utilized to generate 240 additional MRM ion transitions for metabolites screening using Metabolite ID software (Applied Biosystems), including 40 common biotransformation processes. To detect all the metabolites, EMS full scan and precursor scan were also conducted. Only the components detected in the sample and absent in all the control samples were regarded as possible metabolites. To characterize the possible metabolites, both the sample and controls were injected on the LC-MS for EPI and MS^3 scans to obtain their MS^2 and MS^3 spectra. Based on the MS^2, MS^3 spectra of the metabolites and the proposed structures of 17-DMAG fragment ions, the metabolites of 17-DMAG were characterized.

Inhibition of 17-DMAG Oxidative Metabolism by Selective P450 Inhibitors. The incubation mixtures, containing 10 µl of pooled human liver microsomes (20 mg protein/ml) were preincubated in 0.1M phosphate buffer (pH 7.4) in the presence of reduced β-NADPH (1 mM), $MgCl_2$ (3.3 mM) and chemical inhibitor for 3 min at 37°C in a shaking water bath. Parallel control incubations were conducted in the absence of chemical inhibitors. The reactions were initiated by adding 17-DMAG (final concentration 1 µM). The reaction mixtures (final volume 0.2 ml) were incubated for 20 min at 37°C. The P450 isoform-selective inhibitors used were α-naphthoflavone for 1A2 (10 µM), tranylcypromine for 2A6 (1 µM), ticlopidine (10 µM) for 2B6 and 2C19,

quercetin (1 μM) for 2C8, sulfaphenazole (1 μM) for 2C9, quinidine (1 μM) for 2D6, diethyldithiocarbanate (10 μM) for 2E1, and ketoconazole (1 μM) for 3A (Kim et al., 2003; Lee et al., 2006). In positive control experiments, 10 μM α-naphthoflavone inhibited the formation of acetaminophen from phenacetin (20 μM); 1 μM tranylcypromine inhibited the formation of 7-hydroxycoumarin from coumarin (5 μM); 10 μM ticlopidine inhibited the formation of hydroxybupropion from bupropion (50 μM) and formation of hydroxyomperazole from omperazole (50 μM); 1 μM quercetin inhibited the formation of 6α-Hydroxypaclitaxel from paclitaxel (10 μM); 1 μM sulfaphenazole inhibited hydroxytolbutamide formation from tolbutamide (100 μM); 1 μM quinidine inhibited dextrorphan formation from dextromethorphan (5 μM); 10 μM diethyldithiocarbanate inhibited the formation of hydroxychlorzoxazone from chlorzoxazone (50 M); and 1 μM ketoconazole inhibited 1'-hydroxymidazolam formation from midazolam (5 μM) (Lee et al., 2006). The reactions were terminated by adding 400 μl of ice-cold acetonitrile containing 100 ng/ml of MI-63. The samples were vortexed for 30 seconds and centrifuged at 14,000 rpm for 5 min. The supernatant was analyzed by LC-MS/MS to monitor formation rate of 17-DMAG metabolites. The MRM ion transitions for determination of M1, M2, M3, M4 and M6 were 633 → 175, 633 → 322, 603 → 510, 603 → 524, and 665 → 157, respectively. The percentages of inhibition were calculated by the ratio of the amounts of metabolites formed with and without the specific inhibitor.

Incubation with Recombinant CYP450 Enzymes. The incubation mixtures (200 μl), containing 20 pmole recombinant CYP450 enzyme, 0.2 mg reduced β-NADPH, 3.3 mM $MgCl_2$ were preincubated in 0.1M phosphate buffer (pH 7.4) at 37°C in a shaking water

bath. *E. coli* expressed control microsomes without cDNA of human P450 were used as a negative control. The reactions were initiated by adding 17-DMAG (final concentration 1 μM). After incubated for 30 min, the reactions were terminated by adding 400 μl of ice-cold acetonitrile containing 100 ng/ml of MI-63. LC-MS/MS was utilized to monitor formation rate of 17-DMAG metabolites. The formation rates of the metabolites in each CYP450 isozyme were expressed as the percentages relative to their formation rates in CYP3A4.

Results

Relative Percentages of Metabolites in Incubations. The apparent K_m values for the formation of 17-AG from 17-AAG and M1, M3 from 17-DMAG in HLMs were determined as 29.1 μM, 6.61 μM and 7.83 μM, respectively, which were higher than the initial concentrations of 17-AAG and 17-DMAG (5 μM) in stability assays. The relative percentages of GA and 17-AAG and their corresponding hydroquinone and 19-glutathionyl conjugates determined in stability assays were shown in Figure 2. The values were expressed as percentages normalized by peak area ratio of GA or 17-AAG and internal standard at 1 min of incubation. GA exhibited high metabolic stability in HLMs in the absence of reduced GSH (Figure 2A). 73% of GA was not metabolized after 2 h incubation in 1 mg/ml HLMs. 6.4% to 9.3% of GAH_2 was obtained during the course of incubation. Similar amount of GAH_2 was also detected in the incubation with boiled HLMs (negative control), suggesting that the formation of GAH_2 was not dependent on CYP450 enzymes. In contrast, the presence of 5 mM of reduced GSH resulted in the rapid metabolism of GA during the first 5 min of incubation. Only 75.3% and 46.6% of GA remained after incubated for 5 min and 120 min, respectively. Consistently, the reduced GSH resulted in a quick onset of the formation of GAH_2 in HLMs and 85.7% of GAH_2 formed 1 min after the addition of 5 mM reduced GSH. In addition, the formation of GAH_2 was also observed in the incubation of GA and GSH in the absence of HLMs and the peak area ratio of GAH_2 and GA was 1.93 after 2 h incubation. No significant amount of GSH conjugates were detected in all the above incubations using negative MRM ion transitions *m/z* 864 → 821, 866 → 823.

Different from GA, 17AAG was extensively metabolized in 1 mg/ml of HLMs and totally disappeared 45 min after the beginning of incubation (Figure 2B). Less than 1% of 17-$AAGH_2$ was detected during the first 30 min of incubation in HLMs and no 17-$AAGH_2$ was detected after incubation for 1 h. The presence of reduced GSH didn't significantly change the metabolism rate of 17-AAG in HLMs but resulted in a quicker onset of $17AAGH_2$ formation. Furthermore, 3.04% of 17-$AAGH_2$ was obtained when 5 μM of 17-AAG was incubated with 5 mM of reduced GSH for 2 h in the absence of HLMs. GSH conjugates of 17-AAG were not detected over the course of incubations using the negative MRM ion transitions *m/z* 889 → 846 and 891 → 848.

Figure 2C showed the relative percentages of 17-DMAG and its metabolites during the course of incubation. The characterization of 17-DMAG metabolites M1-M7 is discussed in the following section. Compared with 17-AAG, 17-DMAG exhibited improved metabolic stability. 24% of 17-DMAG remained in HLMs after 2 h incubation. Only trace amount (0.24%) of 17-$DMAGH_2$ was obtained after incubation for 2 h. Reduced GSH showed no effect on the metabolism of 17-DMAG and formation of 17-$DMAGH_2$ in HLMs. The maximum percentage (0.33%) of 19-glutathionyl 17-DMAG (17-DMAG-SG) during the incubation was detected at 60 min while 19-glutathionyl 17-DMAG hydroquinone (17-$DMAGH_2$-SG) was not detected during the incubation. In addition, 1.16% of 17-DMAG-SG was obtained when 17-DMAG was incubated with reduced GSH for 2 h in the absence of HLMs.

DMD Fast Forward. Published on December 22, 2010 as DOI: 10.1124/dmd.110.036418
This article has not been copyedited and formatted. The final version may differ from this version.

Identification of 17-DMAG Metabolites. To assign the major fragment ions of protonated 17-DMAG, the MS/MS and MS^3 spectra of GA, 17-AAG and 17-DMAG were obtained. Figure 3A showed the MS/MS spectrum of protonated 17-DMAG. The product ions at *m/z* 58 and 72 of 17-DMAG, which were not detected in the MS/MS spectra of GA and 17-AAG, were assigned to the *N, N*-dimethylethanamine and trimethylamine moieties of 17-dimethylaminoethylamino side chain (Figure 3B). Both product ions at *m/z* 187 and 159 were detected in MS/MS spectra of GA, 17-AAG and 17DMAG. Based on accurate mass measurement, the product ion at *m/z* 187 was assigned to $C_{1\text{-}10}$ as shown in Figure 3B (Lang et al., 2007). On the MS^3 spectra, the ion at *m/z* 187 was further fragmented to generate ions at *m/z* 159, 131 and 117 and their structures were tentatively proposed in Figure 3B.

Besides 17-DMAGH_2 and 17-DMAG-SG, 12 metabolites of 17-DMAG were detected in the HLM incubation but not in negative controls by MS full scan and MRM scan. Three metabolites had a protonated molecular ion (Mr) of 665; five had an Mr of 633; one had an Mr of 627; one had an Mr of 615 and two had an Mr of 603. The major metabolites were the two compounds with an Mr of 603, five compounds with an Mr of 633 and one compound with an Mr of 665. The metabolites with Mr of 603 and 633 were also previously observed in the bile of rats administered with 17-DMAG although their structures were not identified (Egorin et al., 2002).

Five components were detected in the LC-MS/MS chromatogram (*m/z* 633) of HLM incubation extract but not the negative controls (Figure 4A). The protonated molecular

DMD Fast Forward. Published on December 22, 2010 as DOI: 10.1124/dmd.110.036418
This article has not been copyedited and formatted. The final version may differ from this version.

ions (*m/z* 633) of each metabolites showed a mass shift of 16 Da compared with protonated 17-DMAG, indicating the addition of one oxygen. The MS/MS spectrum (Figure 4B) of the component eluted at 8.21 min (M1) showed the product ions at *m/z* 58 and 72, suggested that the oxidation didn't occurred at the 17 side chain. The product ions of M1 at *m/z* 203, 175, 147 and 133 exhibited a mass shift of 16 Da compared with the corresponding product ions of 17-DMAG, indicating that one hydroxyl group generated on $C_{1\text{-}10}$. Furthermore, MS^3 spectrum of protonated M1 (*m/z* 617→203) showed no neutral loss of water from the ion at *m/z* 203, indicating that there was no hydrogen on the carbon next to the hydroxylated carbon. Hence, the hydroxyl of M1 was tentatively assigned to C_{23}. Product ions at *m/z* 187 and 159 were detected in the MS/MS spectrum (Figure 4C) of the component eluted at 9.04 min (M2), suggesting that the hydroxylation did not occur at $C_{1\text{-}10}$ moiety. The detection of a product ion at *m/z* 70 instead of 72 suggested the oxidation on *N, N*-dimethylethanamine while the presence of a product ion at *m/z* 58 indicated that the trimethylamine moiety was intact. Hence, the hydroxyl was tentatively assigned to the α-carbon. The product ion at *m/z* 70 was proposed to be generated from α-hydroxylated 17-DMAG by cleaving the bond between nitrogen and α-carbon, followed by dehydration. Similar α-hydroxylation on 17 side chain was also observed in the metabolism of 17-AAG in HLMs (Lang et al., 2007).

The metabolite eluted at 7.14 min (Figure 4A) showed similar profile of product ions as that of M2 except its product ion at *m/z* 72 instead of *m/z* 70. The major product ions of this metabolite were ions at m/z 159 and 187 instead of ions at *m/z* 322 and 304. The metabolite probably formed by the hydroxylation of C25 or the nitrogen adjacent to C17.

The metabolites eluted at 6.71min and 7.53 min exhibited the same MS/MS pattern and the major product ions were ions at *m/z* 572, 540, 306, 274, 246 and 192 and 177, suggesting the oxidation might occurred at C_{1-10} moiety, C22, C24 or two methoxyl groups. The components eluted at 9.65 min and 10.14 min might not be metabolites since they were also detected in the negative controls. A complete separation of the peaks at 7.53 min and 7.80 min on the chromatogram was not obtained. The structure of the metabolite at 7.80 min was not able to be identified due to the low intensities of its product ions.

Two metabolites with the identical protonated molecular ion at *m/z* 603 (parent - 14) were eluted at 7.57 min (M3) and 7.13 min (M4). Both metabolites were likely formed by demethylation (Figure 5A). The two metabolites had similar MS/MS fragmentation pattern except for the detection of product ions of M3 at *m/z* 571 and 510 and product ions of M4 at *m/z* 585 and 524 (Figure 5B and D). The ion at *m/z* 571 and 510 were derived from protonated M3 by the loss of methanol and subsequent loss of carbamic acid from C_7. Compared with the loss of methanol from C_{12}, the loss of methanol from C_6 position was more energetically favored because it would increase the amount of conjugation in the ansamycin ring. Hence, the product ion of M3 at *m/z* 571 was generated by the loss of methanol from C_6 and M3 was produced by the demethylation from the methoxyl at C_{12} of 17-DMAG (Figure 5C). Similarly, the product ions of M4 at *m/z* 585 and 524 were generated by the loss of water from C_6 and subsequent loss of carbamic acid from C_7 (Figure 5D). M4 was generated by the demethylation from the

DMD Fast Forward. Published on December 22, 2010 as DOI: 10.1124/dmd.110.036418
This article has not been copyedited and formatted. The final version may differ from this version.

methoxyl at C_6. The component eluted at 8.08 min was also detected in the negative controls, indicating that it was not a metabolite of 17-DMAG.

One metabolite eluted at 8.4 min (M5) exhibited a protonated molecular ion at *m/z* 615 (parent - 2), indicating a loss of H_2O from hydroxylized 17-DMAG (Figure 6A). The detection of *m/z* 187 suggested that the metabolism did not occur on $C_{1\text{-}10}$ position. The ions at *m/z* 72 and 58 were not detected in the MS/MS spectrum of M5, suggesting that the metabolism was likely to occur on *N, N*-dimethylethanamine moiety. The base product ion peak of protonated M5 at *m/z* 304 was also detected in the MS/MS spectrum of M2 (Figure 4C). Hence, M5 is proposed to be derived from M2 by the loss of H_2O, which resulted in the formation of a carbon-nitrogen double bond and increased amount of conjugation in the system (Figure 6A).

It is worth to note that the product ion at *m/z* 306 was detected in the MS/MS spectra of M1 (Figure 4B), M3 (Figure 5B), and M4 (Figure 5C). Its counterpart ion at *m/z* 322 in MS/MS spectrum of M2 (Figure 4C) showed a mass shift of 16 Da. Another counterpart ion at *m/z* 304 in MS/MS of M5 (Figure 6A) showed a mass shift of 2 Da. Hence, the ion at *m/z* 306 was possibly generated by the loss of methanol (M1 and M4) or H_2O (M3) from C_{12} and subsequent cleavage of the amide bond in the ring and the bond between C_{10} and C_{11} (Figure 4C). MS^3 spectrum of M3 (*m/z* 633 → 306) showed that the ion at *m/z* 306 generated its fragment ions at *m/z* 274, 246, 229 and 218 (Figure 5B) by the loss or sequential losses of CH_3OH, CO and NH_3 (Figure 5C). The product ion of M2 at

m/z 322 (Figure 4C) and product ion of M5 at *m/z* 304 (Figure 6A) were produced through similar fragmentation.

The metabolite eluted at 6.8 min (M6) showed a protonated molecular ion at *m/z* 665 (parent + 48), indicating the addition of the three oxygen to 17-DMAG. The detection of ion at *m/z* 338 (Figure 6B), a counterpart of the ion at *m/z* 306 of M3 and M4 (a mass shift of 32 Da), indicated that two oxygen atoms were added to C_{11-20} moiety. The presence of the ion at *m/z* 58 suggested that two *N*-methyl groups were not oxidized. Two hydroxyl groups were tentatively assigned to the α-carbon of 17 side chain and C_{25} respectively. The product ions of M6 at *m/z* 185 and 157 (Figure 6B) exhibited a mass shift of 2 Da from their counterpart ions of 17-DMAG at *m/z* 187 and 159, respectively, indicating a third hydroxyl group located at C_{1-10} moiety of M6 and this hydroxyl was readily to be deprived from protonated M6 through dehydration. Hence, the third hydroxyl was tentatively assigned to C_{24} since the formation of a double bond between C_{24} and C_{10} would increase the amount of conjugation and stabilize the product ions of M6. The relative amounts of the six metabolites M1-6 in HLM incubation during 1-120 min were shown in Figure 2C. The relative amounts of 17-DMAG metabolites at 60 min were M3 (2.19%) > M1 (1.48%) > M6 (1.40%) > M2 (1.38%) > M4 (0.98%) > M5 (0.52%) > 17DMAGH_2 (0.19%).

One minor metabolite eluted at 9.2 min exhibited a protonated molecular ion at m/z 627, a mass shift of 10 Da from the counterpart ion of 17-DMAG. The major product ion of this metabolite included ions at m/z 566, 538 and 331. The product ion at m/z 566 was

DMD Fast Forward. Published on December 22, 2010 as DOI: 10.1124/dmd.110.036418
This article has not been copyedited and formatted. The final version may differ from this version.

derived from the protonated molecular ion by the loss of carbamic acid. A subsequent neutral loss of 28 Da instead of 32 Da (the loss of methanol C_{12} or C_6) from m/z 566 was detected and gave rise to m/z 538, suggesting the possible loss of an ethylene or carbon monoxide. Due to the low concentration of this metabolite in HLM incubation, the MS^3 spectra of its product ion were not able to be obtained. Further study is required to definitely identify the structure of the metabolite.

Inhibition of 17-DMAG Oxidative Metabolism by Selective P450 Inhibitors. Identification of the P450 isozymes responsible for oxidative metabolism of 17-DMAG was performed using both P450 selective inhibitors. The results of experiments using specific P450 inhibitors to prevent the formation of 17-DMAG metabolites in HLMs were summarized in Figure 7. The formation of M1, M2, M3, M4 and M6 in HLMs was dramatically inhibited by CYP3A inhibitor. 1 μM ketoconazole resulted in 75-88% inhibition on the formation of the five metabolites. The other inhibitors did not cause remarkable inhibition on the formation of metabolites in HLMs. Results from positive control experiments confirmed that the incubations were performed under optimum conditions.

Oxidative Metabolism of 17-DMAG by Recombinant P450 Isoemzymes. 17-DMAG (1 μM) was incubated with recombinant human P450 Isozymes and the relative formation rates (% of that of CYP3A4) of M1, M2, M3, M4 and M6 were shown in Figure 8. Among the CYP450 isoforms tested, CYP3A4 produced the highest formation rates of M1, M2, M3, M4 and M6. CYP3A5 showed a lower activity for the metabolism of 17-DMAG relative to CYP3A4. CYP2C8, 2D6, 2A6, 2C19 and 1A2 produced M6 at

moderate rates compared with CYP3A4 and 3A5. Other CYP450 enzymes didn't metabolize 17-DMAG at an appreciable rate. The incubation of 17-DMAG with *E. coli* expressed control microsomes didn't show the formation of the metabolites.

DMD Fast Forward. Published on December 22, 2010 as DOI: 10.1124/dmd.110.036418
This article has not been copyedited and formatted. The final version may differ from this version.

Discussion

The molecular modeling analysis showed that the reduction of quinone into hydroquinone facilitated the formation of two more hydrogen bonds between GAH_2 and Hsp90, resulted in a tighter binding between GAH_2 and Hsp90 (Lang et al., 2007). GSH plays an important role in the detoxification of reactive drugs and metabolites formed by hepatic drug metabolizing enzymes (Satoh, 1995). GA and its analogues were observed to react chemically (i.e., nonenzymatically) with GSH to form GSH conjugates at 19-position and the GSH conjugation could be important for the toxicity of GA and its analogues (Cysyk et al., 2006). One objective of this study was to detect and compare the quinone-hydroquinone conversion and GSH conjugation among GA, 17-AAG and 17-DMAG in HLM incubations. Previous study (Lang et al., 2007) and our preliminary study showed that only trace amounts of hydroquinone metabolites and 19-glutathionyl metabolites of 17-AAG or 17-DMAG formed in the HLM incubation. To generate enough metabolites, a substrate concentration of 5 μM and a HLM concentration of 1 mg/ml were selected for metabolic stability assays. The substrate concentration was lower than the K_m values for the formation of major metabolites of 17-AAG and 17-DMAG. To evaluate the formation of GSH conjugates of GA derivatives in HLMs, GSH in reduced form was added to the HLM incubations to reach a final concentration of 5 mM as described previously (Lang et al., 2007; Guo et al., 2008). It was also reported (Guo et al., 2008) that only less than 15% of 17-AAG-SG formed even after 24 h of incubation in the presence of 5 mM of reduced GSH, indicating a slow GSH conjugation rate. Hence, the total incubation time of metabolic stability assays was chosen as 2 h to acquire as

high amount of GSH conjugates as possible while maintaining reasonable enzyme activity.

6.4% to 9.3% of GAH_2 was detected in HLM incubation in the absence of GSH, much lower than the amount (40-73%) detected in a published report (Lang et al., 2007). The inconsistency might be partially caused by oxygen exposure during sample preparation as some GAH_2 was oxidized into GA. The reduced GSH stimulated the reduction of GA and 78-88% of GAH_2 was detected, which was consistent with the amount of GAH_2 obtained in HLM incubation under hypoxic conditions(Lang et al., 2007). The reduction of GA was not dependent on CYP450 enzymes since the incubation of GA with GSH in the absence of HLMs produced more GAH_2 than the incubation in the presence of HLMs. In contrast, reduced GSH did not enhance the formation of 17-$AAGH_2$ and 17-$DMAGH_2$ in HLMs. Less than 1% of 17-$AAGH_2$ and 17-$DMAGH_2$ formed in HLM incubations. This agreed well with a previous study (Lang et al., 2007) in which only 2% of 17-$AAGH_2$ was detected after incubation in HLMs for 60 min. The reason for different formation rates of GAH_2 and 17-$AAGH_2$ in HLMs has been discussed: 17-allylamino group of 17AAG is a stronger electron-donating substituent than the 17-methoxy of GA, leading to a more negative shift in one-electron redox potential for 17AAG. As a result, 17AAG is not as easily reduced as GA (Lang et al., 2007). Similarly, 17-dimethylaminoethylamino is also a stronger electron-donating substituent than the 17-methoxy, resulting the slower formation of 17-$DMAGH_2$ than GAH_2. Considering the tight binding between GAH_2 and Hsp90, the tendency to get reduced might result in a higher nonselective toxicity of GA than that of 17-AAG and 17-DMAG.

GA, 17-AAG and 17-DMAG were reported to react chemically with GSH to form GSH conjugates at 19-position (Cysyk et al., 2006). However, in current study, only 0.33% of 17-DMAG-SG formed in the incubation of 17-DMAG with GSH in the presence of HLMs and 1.16% of 17-DMAG-SG formed in the absence of HLMs. The presence of proteins in the incubation might decrease GSH conjugation. Consistent with previous *in vitro* and *in vivo* studies (Egorin et al., 1998; Lang et al., 2007), no significant amount of GSH conjugates of 17-AAG were detected. Similarly, the GSH conjugates of GA were not detected in the presence and absence of HLMs.

Quinone/hydroquinone cycling was proposed to be the primary metabolism pathway of GA and its analogues (Guo et al., 2008). NADPH-dependent redox cycling rates of GA analogues were determined by measuring the oxygen consumption rates: 17-DMAG > GA > 17-AAG, while the GSH conjugation rates are: GA > 17-DMAG > 17-AAG. However, these findings were inconsistent with the rapid *in vitro and in vivo* metabolism of 17-AAG (Egorin et al., 2001; Musser et al., 2003).

Our study showed that benzoquinone reduction and GSH conjugation were not the primary metabolism pathways of 17-DMAG in HLMs. This observation was supported by *in vivo* metabolism data of 17-DMAG in rats (Egorin et al., 2002). In the study, 11 compounds with UV spectra similar to that of 17-DMAG were detected in rat bile after i.v. administration of 17-DMAG. Although the structures of the 11 compounds were not identified, the metabolism did not involve the alterations to the benzoquinone moiety

because their UV spectra were not altered compared with 17-DMAG. Among the 11 metabolites, four had Mr of 633 and two had Mr of 603, which were also detected in our HLM incubations.

The results of metabolite identification revealed that the biotransformation of 17-DMAG by CYP450 enzymes differed from that of 17-AAG. The extensive oxidative metabolism of 17-AAG on the 17-allylamino side chain resulted in the formation of 17-AG as well as epoxide and diol metabolites (Egorin et al., 1998). The hydroxylation on C_{22} and demethylation from methoxy moieties were detected as the minor biotransformation pathways of 17-AAG in HLMs (Lang et al., 2007). In contrast, the hydroxylation on C_{23} (M1) and demethylation from methoxy moieties (M3 and M4) were the primary biotransformation of 17-DMAG in HLMs (Figure 8). Similar to 17-AAG, the hydroxylation of the adjacent carbon to the nitrogen generated a stable carbinolamine intermediate (M2). Subsequently, M2 underwent the loss of H_2O and formed an imine metabolite (M5). Usually, carbinolamines are known as unstable intermediates in *N*-demethylation. Most carbinolamines tend to form imine intermediates by the loss of water or decompose into dealkylated amine by the loss of aldehyde or ketone. However, stable carbinolamines and imines exist in aqueous solutions under some specific circumstances. For example, carbinolamines and imines can be stabilized by adjacent electron-withdrawing groups (Upthagrove and Nelson, 2001). Furthermore, a stable carbinolamine, hydroxymethylpentamethylmelamine, was detected as a metabolite in mouse plasma (Abikhalil et al., 1986) and rat liver microsomes (Ames et al., 1983) because the adjacent substituents delocalize the lone pair nitrogen electrons and

stabilize the carbinolamine. Additionally, stable carbinolamines have been isolated or detected as metabolites to a number of drugs including benzamides (Huizing et al., 1980), carbamates (Dorough and Casida, 1964), procarbazine (Weinkam and Shiba, 1978), N-methylcarbazole (Ebner et al., 1991), medazepam (Schwartz and Kolis, 1972), verapamil (Walles et al., 2002), pyrimidinyl-pyridopyrazines (Prakash and Soliman, 1997), and ecabapide (Fujimaki et al., 1995). Quinone is known as an electron-withdrawing group by resonance (Hiramatsu et al., 1983). The presence of the quinone adjacent to the nitrogen in M2, M5 and M6 of 17-DMAG allows the delocalization of the lone pair nitrogen electrons and stabilizes the metabolites.

17-AAG was a known substrate of CYP3A4 (Lang et al., 2007). In the current study, the reaction phenotyping experiments using recombinant human P450s and selective P450 chemical inhibitors revealed that CYP3A4 and CYP3A5 were the major P450 isozymes responsible for the oxidative metabolism of 17-DMAG in HLMs. In addition, CYP2C8, 2D6, 2A6, 2C19 and 1A2 were observed to contribute to the formation of M6. Based on the identified metabolite profiles, the *in vitro* oxidative biotransformation pathways for 17-DMAG in HLMs were proposed (Figure 9).

In conclusion, this study tentatively characterized six oxidative metabolites of 17-DMAG in HLMs and revealed that the primary biotransformations of 17-DMAG in HLMs were hydroxylation and demethylation on its side chains. CYP3A4 and CYP3A5 were identified as the major P450 isozymes responsible for the oxidative metabolism of 17-DMAG in HLMs. The metabolic data generated in the current study have important

implications for the discovery of more metabolically stable and less toxic geldanamycin analogs for the treatment of solid tumors.

Authorship Contribution

NZ and PZ was involved in the study design, study execution, data collection and analyses, and writing and editing all aspects of this manuscript. NZ and PZ contributed equally to this work. SW participated in research design and contributed to the analytical tools. DS was involved in the study design, data collection and analyses, as well as the editing of all aspects of this manuscript.

References

Abikhalil F, Dubois J, Hanocq M and Atassi G (1986) A New Algorithm for Computing the Parameters of Linear Compartment Models in Pharmacokinetics. *European Journal of Drug Metabolism and Pharmacokinetics* **11:**51-59.

Ames MM, Sanders ME and Tiede WS (1983) Role of N-Methylolpentamethylmelamine in the Metabolic-Activation of Hexamethylmelamine. *Cancer Research* **43:**500-504.

An WG, Schnur RC, Neckers L and Blagosklonny MV (1997) Depletion of p185(erbB2), Raf-1 and mutant p53 proteins by geldanamycin derivatives correlates with antiproliferative activity. *Cancer Chemotherapy and Pharmacology* **40:**60-64.

Cysyk RL, Parker RJ, Barchi JJ, Jr., Steeg PS, Hartman NR and Strong JM (2006) Reaction of geldanamycin and C17-substituted analogues with glutathione: product identifications and pharmacological implications. *Chem Res Toxicol* **19:**376-381.

Dorough HW and Casida JE (1964) Nature of Certain Carbamate Metabolites of Insecticide Sevin. *Journal of Agricultural and Food Chemistry* **12:**294-&.

Ebner T, Meese CO and Eichelbaum M (1991) Regioselectivity and Stereoselectivity of the Metabolism of the Chiral Quinolizidine Alkaloids Sparteine and Pachycarpine in the Rat. *Xenobiotica* **21:**847-857.

Egorin MJ, Lagattuta TF, Hamburger DR, Covey JM, White KD, Musser SM and Eiseman JL (2002) Pharmacokinetics, tissue distribution, and metabolism of 17-(dimethylaminoethylamino)-17-demethoxygeldanamycin (NSC 707545) in CD2F1 mice and Fischer 344 rats. *Cancer Chemotherapy and Pharmacology* **49:**7-19.

Egorin MJ, Rosen DM, Wolff JH, Callery PS, Musser SM and Eiseman JL (1998) Metabolism of 17-(allylamino)-17-demethoxygeldanamycin (NSC 330507) by murine and human hepatic preparations. *Cancer Research* **58:**2385-2396.

Egorin MJ, Zuhowski EG, Rosen DM, Sentz DL, Covey JM and Eiseman JL (2001) Plasma pharmacokinetics and tissue distribution of 17-(allylamino)-17-demethoxygeldanamycin (NSC 330507) in CD2F1 mice1. *Cancer Chemotherapy and Pharmacology* **47:**291-302.

Fujimaki Y, Hosokami T and Ono K (1995) Identification of Urinary Metabolites of Ecabapide in Rat. *Xenobiotica* **25:**501-510.

Glaze ER, Lambert AL, Smith AC, Page JG, Johnson WD, McCormick DL, Brown AP, Levine BS, Covey JM, Egorin MJ, Eiseman JL, Holleran JL, Sausville EA and Tomaszewski JE (2005) Preclinical toxicity of a geldanamycin analog, 17-(dimethylaminoethylamino)-17-demethoxygeldanamycin (17-DMAG), in rats and dogs: potential clinical relevance. *Cancer Chemotherapy and Pharmacology* **56:**637-647.

Goetz MP, Toft D, Reid J, Ames M, Stensgard B, Safgren S, Adjei AA, Sloan J, Atherton P, Vasile V, Salazaar S, Adjei A, Croghan G and Erlichman C (2005) Phase I trial of 17-allylamino-17-demethoxygeldanamycin in patients with advanced cancer. *J Clin Oncol* **23:**1078-1087.

Guo W, Reigan P, Siegel D and Ross D (2008) Enzymatic reduction and glutathione conjugation of benzoquinone ansamycin heat shock protein 90 inhibitors: relevance for toxicity and mechanism of action. *Drug Metab Dispos* **36:**2050-2057.

Guo WC, Reigan P, Siegel D, Zirrolli J, Gustafson D and Ross D (2005) Formation of 17-allylamino-demethoxygeldanamycin (17-AAG) hydroquinone by NAD(P)H : quinone oxidoreductase 1: Role of 17-AAG hydroquinone in heat shock protein 90 inhibition. *Cancer Research* **65:**10006-10015.

Guo WC, Reigan P, Siegel D, Zirrolli J, Gustafson D and Ross D (2006) The bioreduction of a series of benzoquinone ansamycins by NAD(P)H : quinone oxidoreductase 1 to more potent heat shock protein 90 inhibitors, the hydroquinone ansamycins. *Molecular Pharmacology* **70:**1194-1203.

Hiramatsu M, Shiozaki K, Fujinami T and Sakai S (1983) Preparation and Electrochemical Properties of Palladium(0) Complexes Coordinated by Quinones and 1,5-Cyclooctadiene. *Journal of Organometallic Chemistry* **246:**203-211.

Huizing G, Segura J and Beckett AH (1980) On the Mechanism of Metabolic N-Dealkylation - Isolation of a Relatively Stable Carbinolamine. *Journal of Pharmacy and Pharmacology* **32:**650-651.

Hwang K, Scripture CD, Gutierrez M, Kummar S, Figg WD and Sparreboom A (2006) Determination of the heat shock protein 90 inhibitor 17-dimethylaminoethylamino-17-demethoxygeldanamycin in plasma by liquid chromatography-electrospray mass spectrometry. *J Chromatogr B Analyt Technol Biomed Life Sci* **830:**35-40.

Kim KA, Kim MJ, Park JY, Shon JH, Yoon YR, Lee SS, Liu KH, Chun JH, Hyun MH and Shin JG (2003) Stereoselective metabolism of lansoprazole by human liver cytochrome P450 enzymes. *Drug Metab Dispos* **31:**1227-1234.

Lang WS, Caldwell GW, Li J, Leo GC, Jones WJ and Masucci JA (2007) Biotransformation of geldanamycin and 17-allylamino-17-demethoxygeldanamycin by human liver microsomes: Reductive versus oxidative metabolism and implications. *Drug Metabolism and Disposition* **35:**21-29.

Lee HK, Moon JK, Chang CH, Choi H, Park HW, Park BS, Lee HS, Hwang EC, Lee YD, Liu KH and Kim JH (2006) Stereoselective metabolism of endosulfan by human liver microsomes and human cytochrome P450 isoforms. *Drug Metabolism and Disposition* **34:**1090-1095.

McIlwrath AJ, Brunton VG and Brown R (1996) Cell-cycle arrests and p53 accumulation induced by geldanamycin in human ovarian tumour cells. *Cancer Chemotherapy and Pharmacology* **37:**423-428.

Moreno-Farre J, Asad Y, Pacey S, Workman P and Raynaud FI (2006) Development and validation of a liquid chromatography/tandem mass spectrometry method for the determination of the novel anticancer agent 17-DMAG in human plasma. *Rapid Commun Mass Spectrom* **20:**2845-2850.

Musser SM, Egorin MJ, Zuhowski EG, Hamburger DR, Parise RA, Covey JM, White KD and Eiseman JL (2003) Biliary excretion of 17-(allylamino)-17-demethoxygeldanamycin (NSC 330507) and metabolites by Fischer 344 rats. *Cancer Chemotherapy and Pharmacology* **52:**139-146.

Prakash C and Soliman V (1997) Metabolism and excretion of a novel antianxiety drug candidate, CP-93,393, in Long Evans rats - Differentiation of regioisomeric glucuronides by LC/MS/MS. *Drug Metabolism and Disposition* **25:**1288-1297.

Satoh K (1995) The high non-enzymatic conjugation rates of some glutathione S-transferase (GST) substrates at high glutathione concentrations. *Carcinogenesis* **16:**869-874.

Schwartz MA and Kolis SJ (1972) Pathways of Medazepam Metabolism in Dog and Rat. *Journal of Pharmacology and Experimental Therapeutics* **180:**180-&.

Smith NF, Hayes A, Nutley BP, Raynaud FI and Workman P (2004) Evaluation of the cassette dosing approach for assessing the pharmacokinetics of geldanamycin analogues in mice. *Cancer Chemotherapy and Pharmacology* **54:**475-486.

Upthagrove AL and Nelson WL (2001) Carbinolamines, imines, and oxazolidines from fluorinated propranolol analogs. F-19 NMR and mass spectral characterization and evidence for formation as intermediates in cytochrome P450-catalyzed N-dealkylation. *Drug Metabolism and Disposition* **29:**1114-1122.

Walles M, Thum T, Levsen K and Borlak J (2002) Verapamil: new insight into the molecular mechanism of drug oxidation in the human heart. *Journal of Chromatography A* **970:**117-130.

Weinkam RJ and Shiba DA (1978) Metabolic Activation of Procarbazine. *Life Sciences* **22:**937-945.

Footnotes:

This work was partially supported by the National Institutes of Health [Grants RO1 CA120023, R21 CA143474]; and the University of Michigan Cancer Center Research [Grant Munn].

Reprint request to:

Duxin Sun, Department of Pharmaceutical Sciences, College of Pharmacy, The University of Michigan, 428 Church Street, Ann Arbor, MI 48109

Email: duxins@umich.edu

Figure 1. Structures of GA, 17-AAG, 17-DMAG and 17-AG

Figure 2. Relative percentages of (A) GA and GAH_2; (B) 17-GA and 17-GAH_2 and (C) 17-DMAG and its metabolites in the incubations with HLMs in the presence or absence of 5 mM reduced GSH. The values were expressed as percentages normalized by peak area ratio of parent compound and internal standard at 1 min of incubation. * stands for the presence of 5 mM GSH.

Figure 3. (A) MS/MS spectrum and MS^3 spectrum (*m/z* 617 → 187) of protonated 17-DMAG. (B) The proposed fragmentation pathways of protonated 17-DMAG.

Figure 4. (A) LC-MS/MS chromatogram (*m/z* 633) of HLM incubation extract. Five metabolites of 17-DMAG formed by the addition of one oxygen; (B) MS/MS spectrum of the metabolite eluted at 8.21 min (M1); (C) MS/MS spectrum of the metabolite eluted at 9.04 min (M2).

Figure 5. (A) LC-MS/MS chromatogram (*m/z* 603) of HLM incubation extract. Two metabolites of 17-DMAG formed by demethylation; (B) MS/MS spectrum and MS^3 spectrum (*m/z* 603 → 306) of the metabolite eluted at 7.57 min (M3); (C) The porposed formation and fragmentation pathways of the product ion at *m/z* 306; (D) MS/MS spectrum of the metabolite eluted at 7.13 min (M4).

Figure 6. MS/MS spectrum of (A) the metabolite eluted at 8.40 min (M5) and (B) the metabolite eluted at 6.80 min (M6).

Figure 7. Effect of selective CYP450 inhibitors on the oxidative metabolism of 17-DMAG by HLMs.

Figure 8. Relative formation rates of M1, M2, M3, M4 and M6 by recombinant human CYP450 isozymes. The values were expressed as percentages normalized by the formation rate in CYP3A4 incubation.

Figure 9. Summary of *in vitro* oxidative metabolism pathways of 17-DMAD in HLMs.

Figure 1

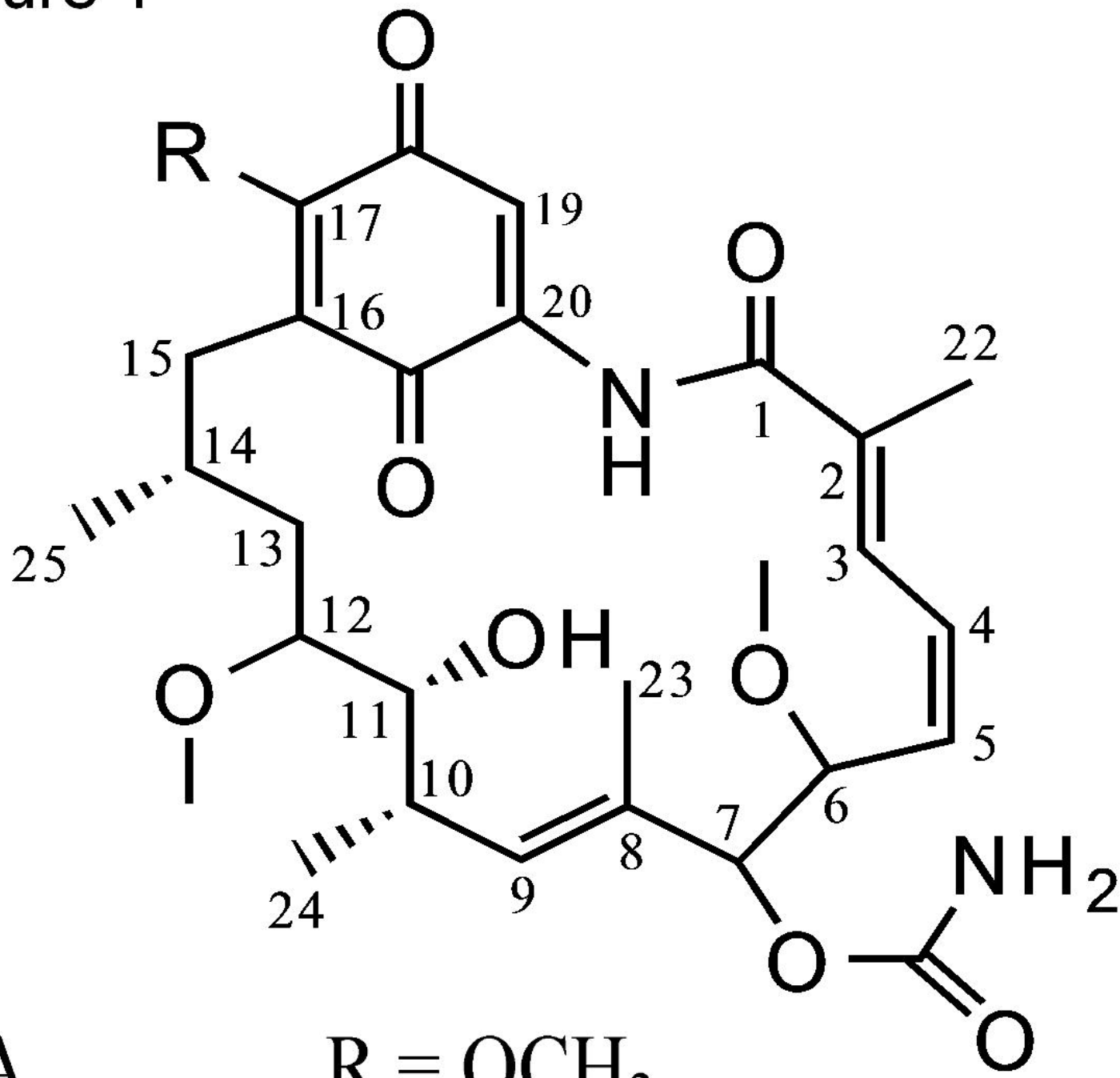

GA $R = OCH_3$

17-AAG $R = NHCH_2CH{=}CH_2$

17-DMAG $R = NHCH_2CH_2N(CH_3)_2$

17-AG $R = NH_2$

Figure 2

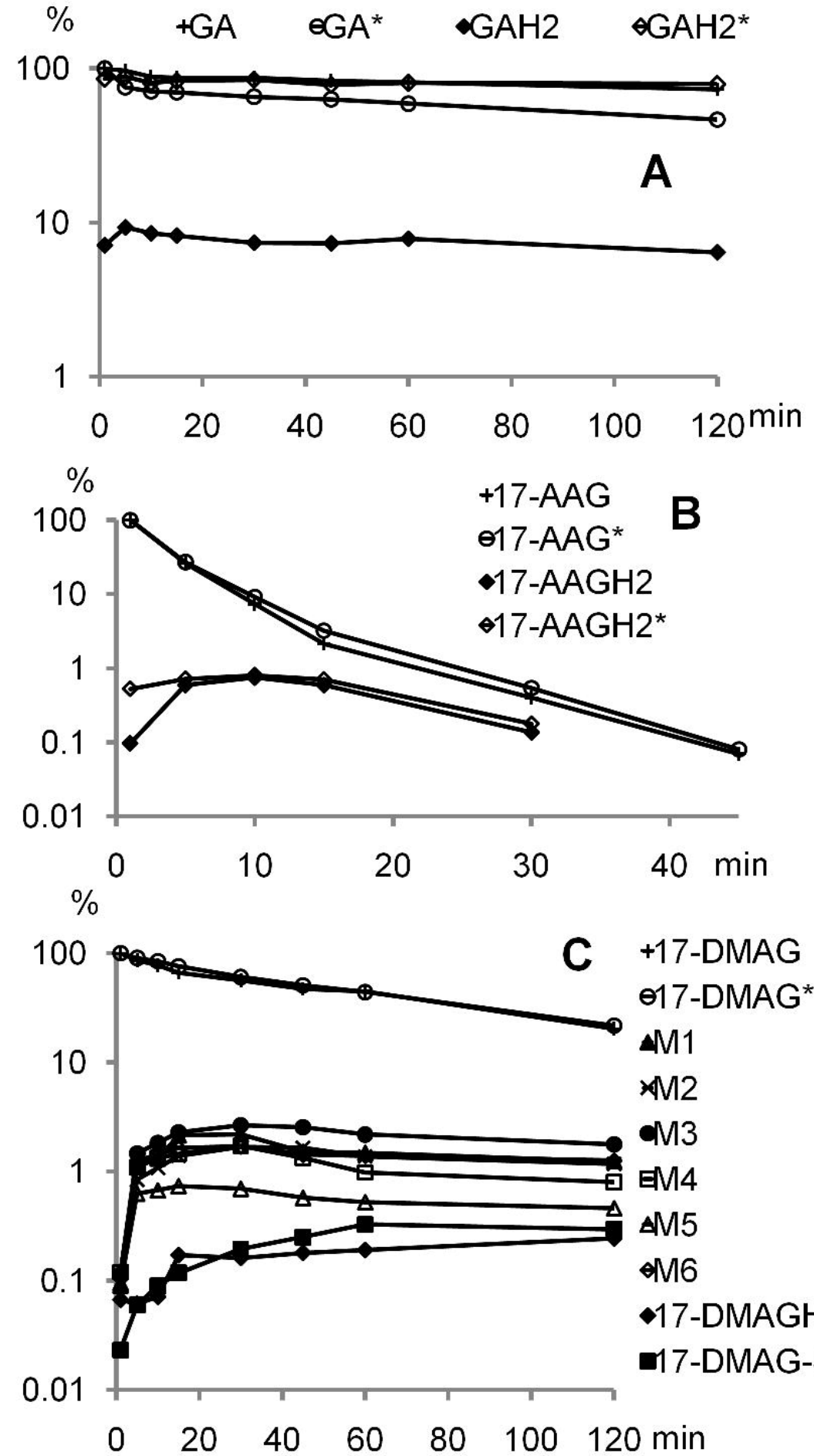
%
+GA
GA*
GAH2
GAH2*
100
10
1
A
0
20
40
60
80
100
120
min
%
+17-AAG
17-AAG*
17-AAGH2
17-AAGH2*
B
100
10
1
0.1
0.01
0
10
20
30
40
min
%
C
+17-DMAG
17-DMAG*
M1
M2
M3
M4
M5
M6
17-DMAGH2
17-DMAG-SG*
100
10
1
0.1
0.01
0
20
40
60
80
100
120
min

Figure 3

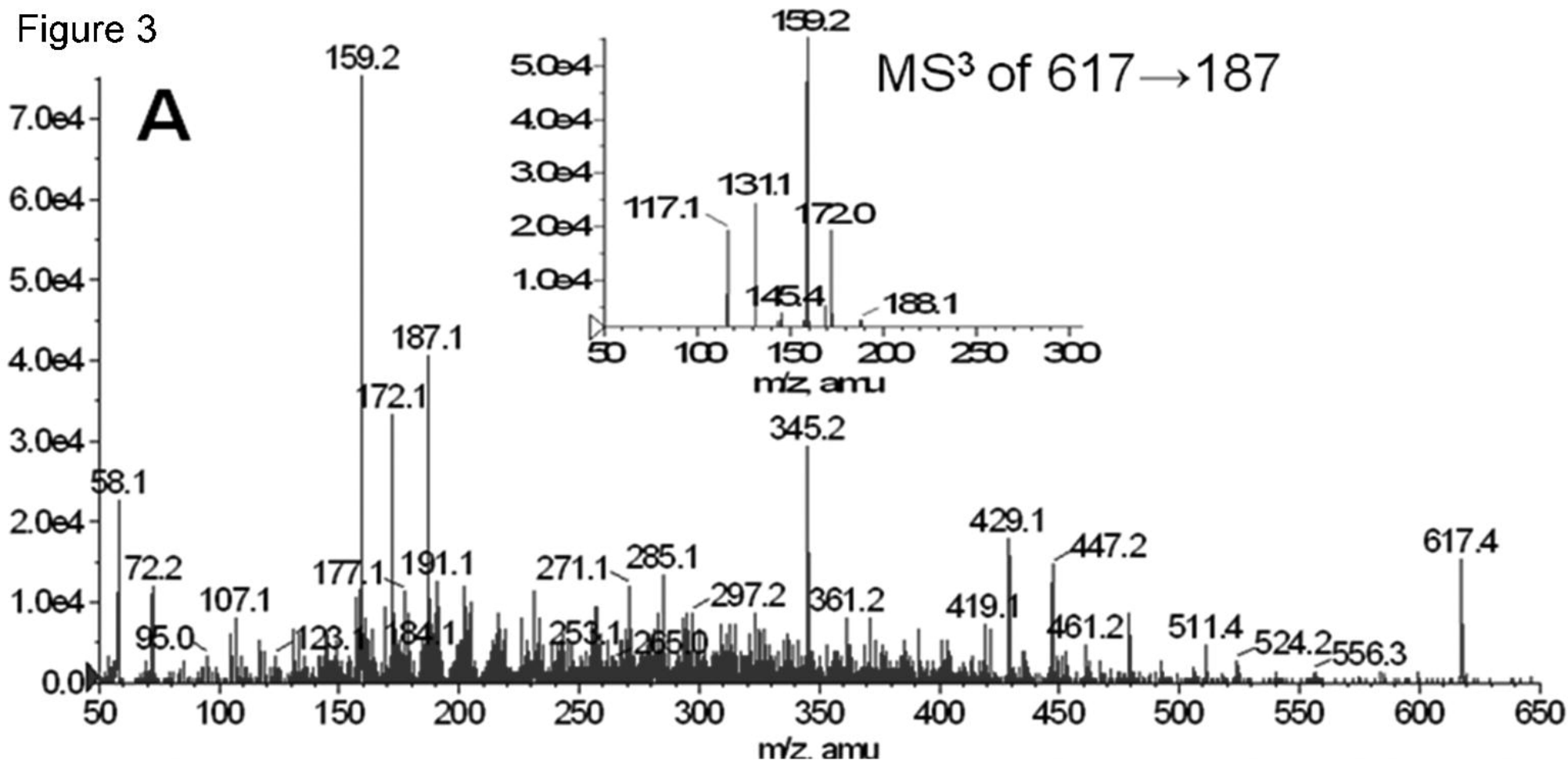
A
MS³ of 617→187
159.2
187.1
172.1
345.2
58.1
72.2
107.1
95.0
177.1
191.1
123.1
184.1
271.1
285.1
253.1
265.0
297.2
361.2
429.1
419.1
447.2
461.2
511.4
524.2
556.3
617.4
m/z, amu
117.1
131.1
172.0
145.4
188.1

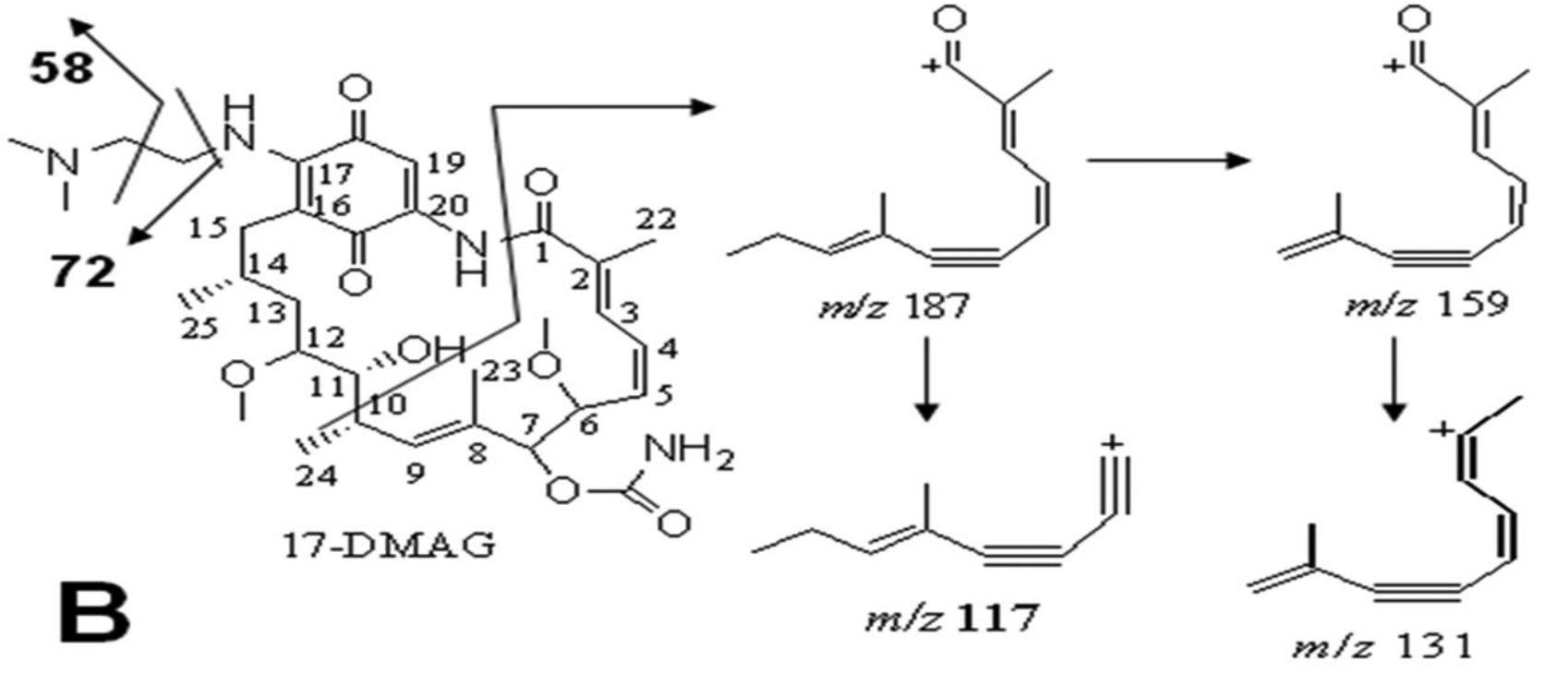
58
72
17-DMAG
m/z 187
m/z 159
m/z 117
m/z 131
B

Figure 4

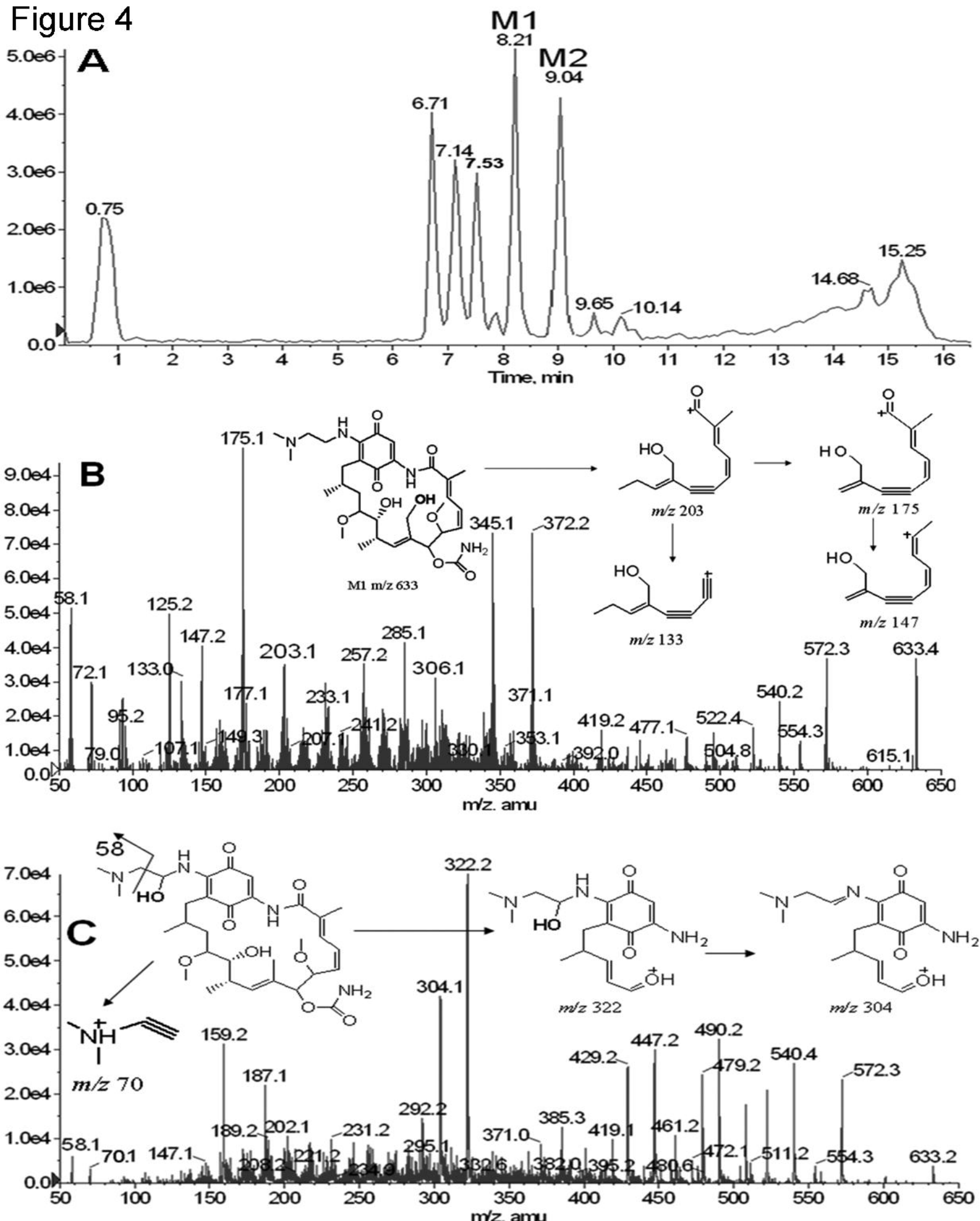
A
M1
8.21
M2
9.04
6.71
7.14
7.53
0.75
15.25
14.68
9.65
10.14
Time, min
B
175.1
345.1
372.2
M1 m/z 633
m/z 203
m/z 175
m/z 133
m/z 147
58.1
125.2
147.2
72.1
133.0
203.1
257.2
285.1
306.1
177.1
233.1
371.1
95.2
419.2
477.1
522.4
540.2
572.3
633.4
554.3
615.1
m/z, amu
C
58
322.2
304.1
m/z 70
m/z 322
m/z 304
159.2
187.1
292.2
447.2
490.2
429.2
479.2
540.4
572.3
m/z, amu

Figure 5

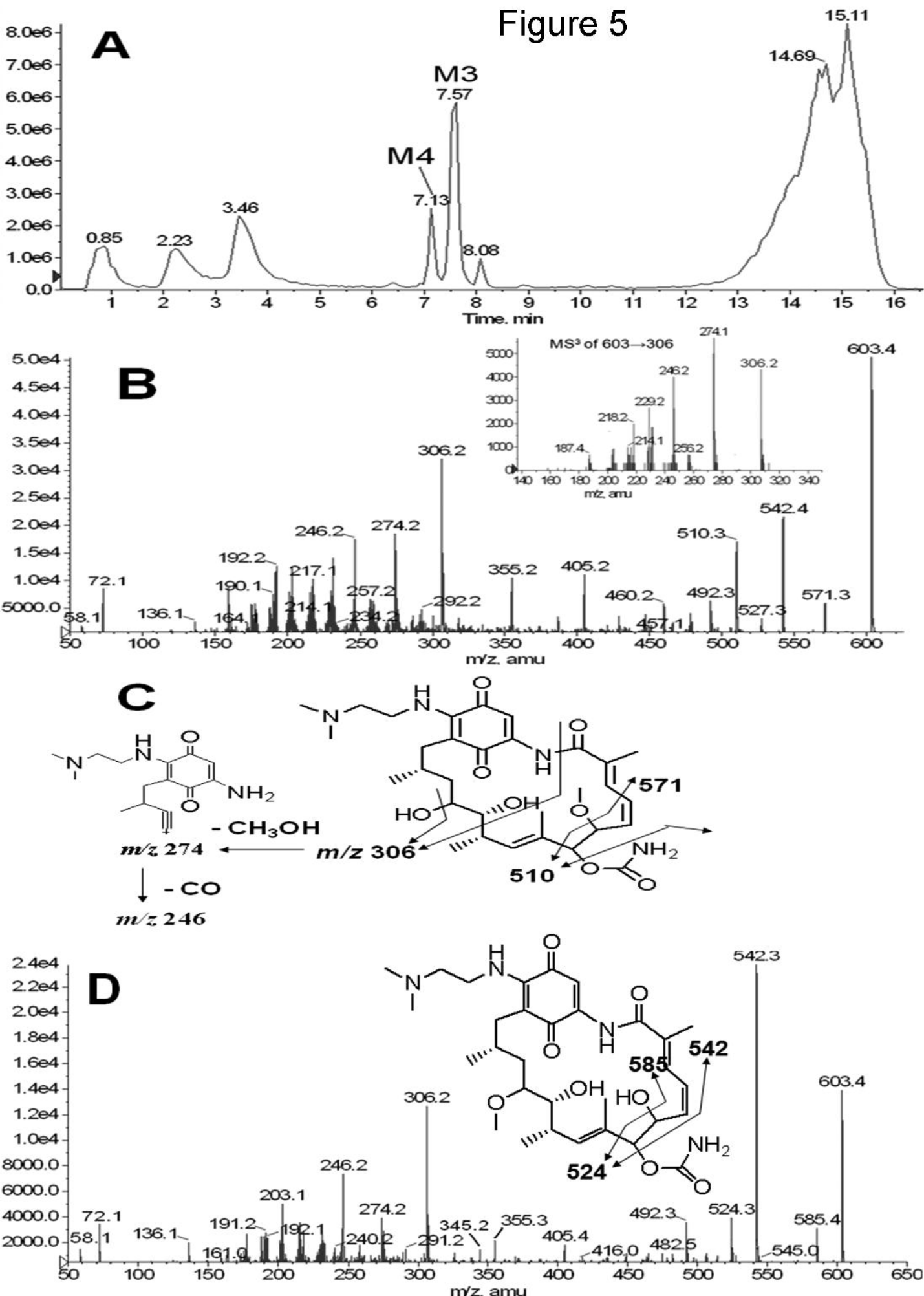
A
M3
7.57
M4
7.13
0.85
2.23
3.46
8.08
14.69
15.11
Time. min
B
MS³ of 603→306
274.1
306.2
246.2
229.2
218.2
214.1
187.4
256.2
603.4
542.4
510.3
492.3
527.3
571.3
355.2
405.2
460.2
457.1
292.2
257.2
246.2
274.2
192.2
217.1
190.1
214.1
72.1
58.1
136.1
164
m/z. amu
C
- CH3OH
m/z 274
- CO
m/z 246
m/z 306
571
510
D
542.3
542
585
603.4
306.2
524
246.2
203.1
274.2
72.1
58.1
136.1
191.2
192.1
161.0
240.2
291.2
345.2
355.3
405.4
492.3
524.3
585.4
416.0
482.5
545.0
m/z. amu

Figure 6

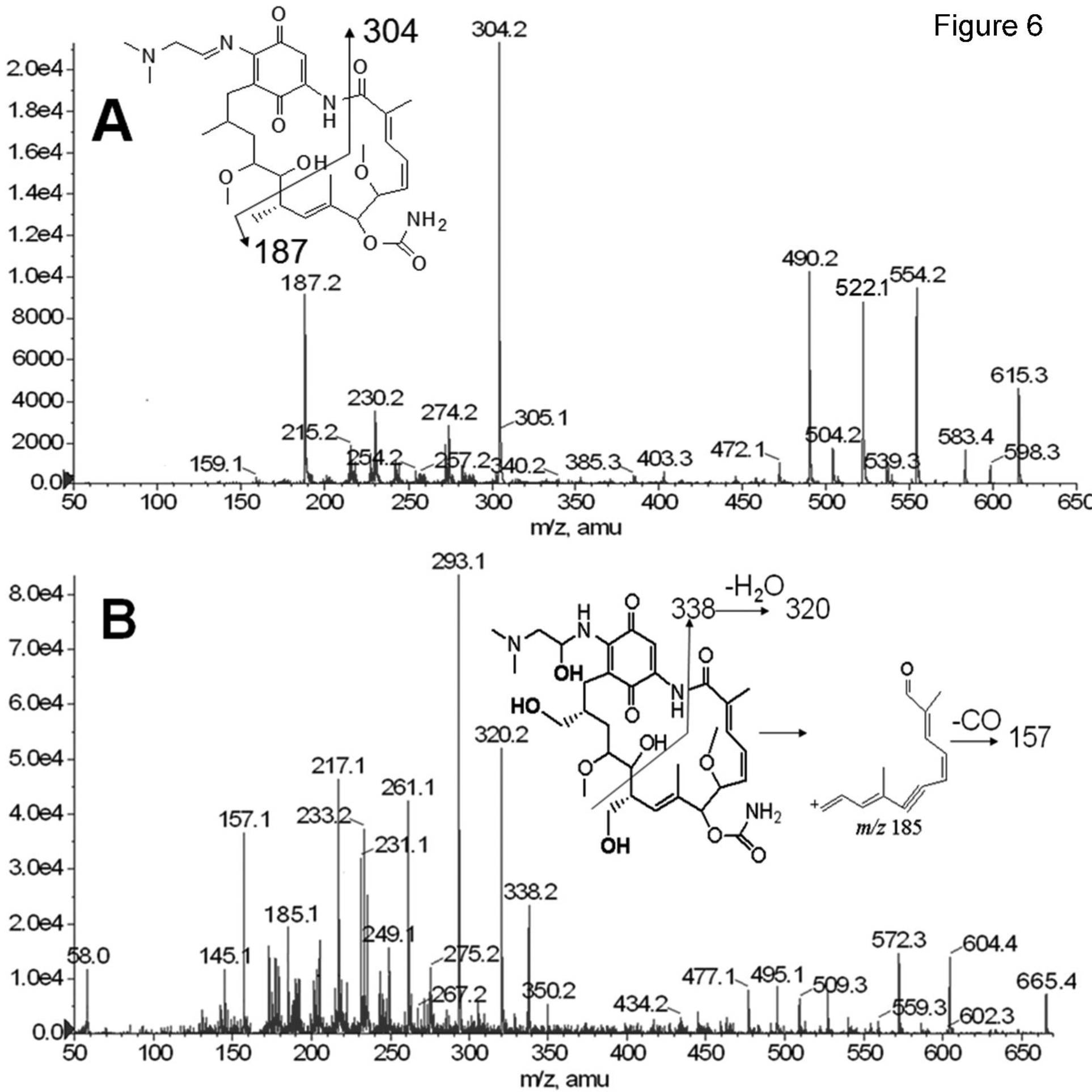
A
304
187
304.2
187.2
490.2
522.1
554.2
615.3
230.2
274.2
305.1
215.2
504.2
583.4
598.3
159.1
254.2
257.2
340.2
385.3
403.3
472.1
539.3
m/z, amu
B
293.1
-H2O
338
320
320.2
217.1
261.1
157.1
233.2
231.1
338.2
185.1
249.1
58.0
145.1
275.2
267.2
350.2
572.3
604.4
477.1
495.1
509.3
665.4
434.2
559.3
602.3
-CO
157
m/z 185
m/z, amu

Figure 7

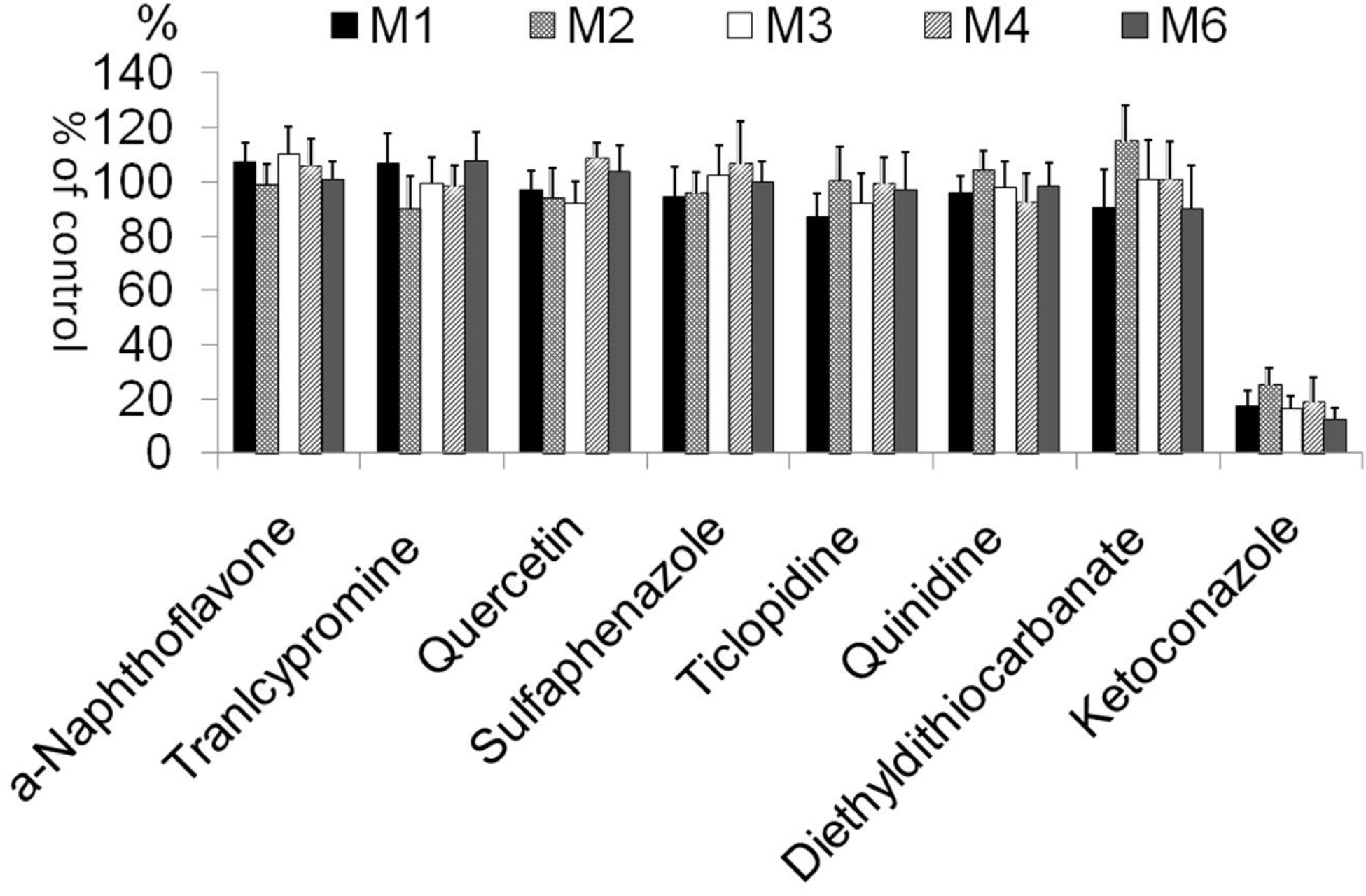
%
M1
M2
M3
M4
M6
140
120
100
80
60
40
20
0
% of control
a-Naphthoflavone
Tranlcypromine
Quercetin
Sulfaphenazole
Ticlopidine
Quinidine
Diethyldithiocarbanate
Ketoconazole

Figure 8

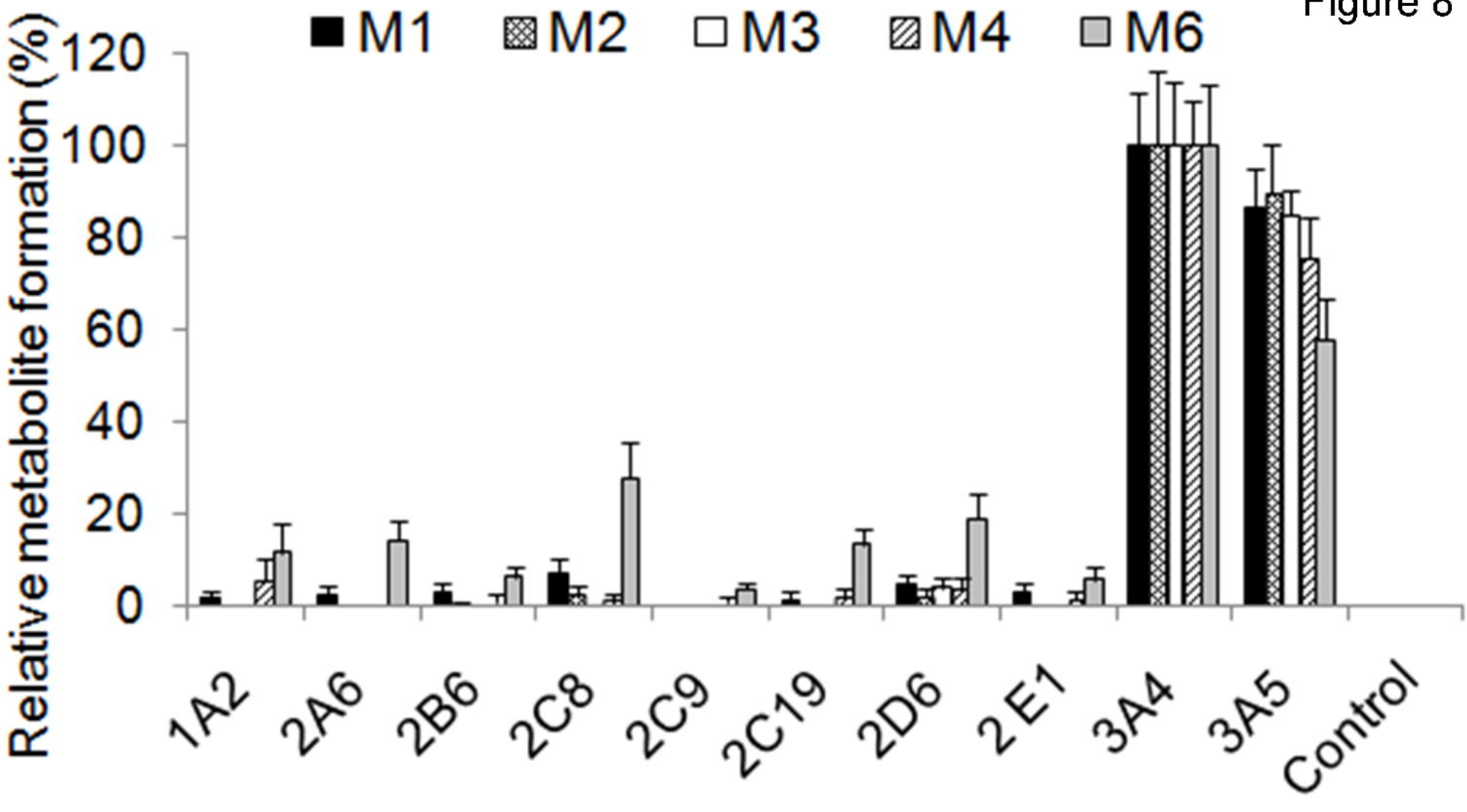
M1
M2
M3
M4
M6
Relative metabolite formation (%)
120
100
80
60
40
20
0
1A2
2A6
2B6
2C8
2C9
2C19
2D6
2E1
3A4
3A5
Control

Figure 9

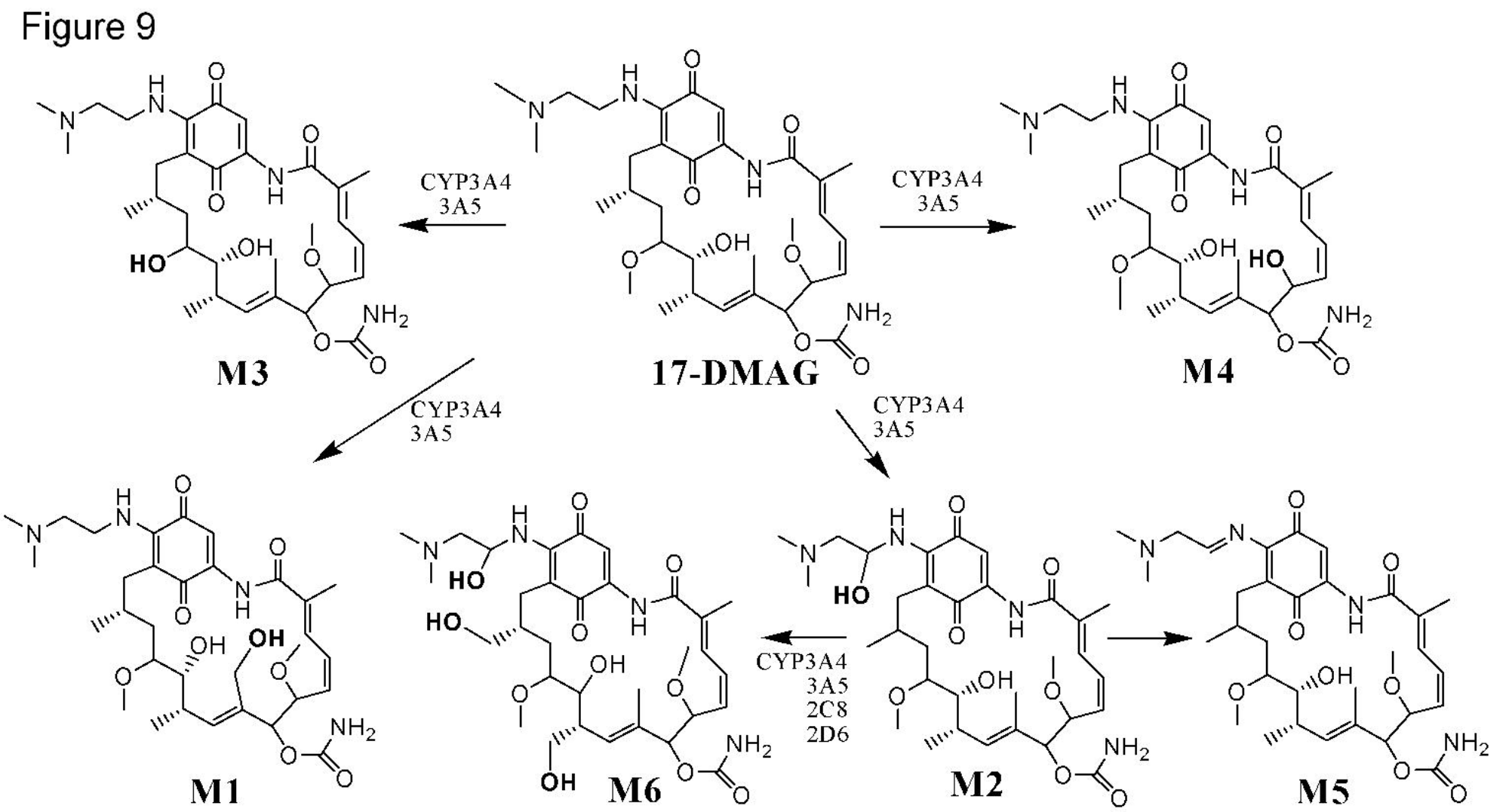
CYP3A4
3A5
CYP3A4
3A5
CYP3A4
3A5
CYP3A4
3A5
CYP3A4
3A5
2C8
2D6
M3
17-DMAG
M4
M1
M6
M2
M5